INTERNATIONAL JOURNAL FOR NUMERICAL METHODS IN FLUIDS, VOL. 16, 217–230 (1993)

COMPUTER SIMULATION OF MOIST ATMOSPHERIC CONVECTION WITH FINITE ELEMENTS

KENNETH J. MANN

Department of Mathematics, Monash University, P.O. Box 197, Caulfield East, Victoria 3145, Australia

SUMMARY

A computer simulation is made of cellular convection in a moist atmosphere in an endeavour to obtain a computer model which more closely approximates the observed modes of convection. A finite element Galerkin technique, with Taylor approximation and Crank–Nicolson, is employed and comparisons are made with the author's earlier finite element models of convection in an absolutely unstable atmosphere and with finite difference models. It is found that the inclusion of the moisture effects alters the structure of a cell to that of a narrow ascending region and a wider descending region with the former of larger velocities than the latter, and also alters the preferred mode of convection by increasing the aspect ratio. This more closely resembles that which is observed in the atmosphere.

KEY WORDS Finite elements Moist atmosphere Convection Computation

INTRODUCTION

Agee and Dowell[1] have recorded that observational studies of mesoscale cellular convection indicate that the aspect ratios are typically of the order of 20. Mathematical and laboratory models have not been able to simulate this. It is possible that important physical mechanisms which tend to broaden the cell geometry are absent from the absolutely unstable model. A non-linear finite element study is made of moist atmospheric convection to determine, principally, the effect of the moisture inclusion on the aspect ratio and the cell structure and also to understand some of the properties of the inclusion of the moisture. The moist model of Van der Borght and Agee[2] imposed the observed aspect ratio through an averaging technique and obtained the appropriate convection but the reverse has not been attained.

Satellite photographs, as depicted in Agee and Dowell[1] and others, show cumulus convection occurring as a tesselation of cells in some polygonal plan, which many observers classify as hexagonal, an assumption which has been found to be quite appropriate as evidenced in the results of the mathematical model of Van der Borght and Agee.[2] A two-dimensional mathematical model similar to that of this research has been used by Sheu *et al.*[3] to gain some insight into the physical processes of the dynamics of these cells. They used a finite-difference algorithm to effect solutions.

Observations also indicate that convective clouds are aligned parallel to the vertical wind shear.[4] This conclusion agrees with the laboratory experiment[5] and the theory[6] which show the Benard convection cells in the fluid layer heated from below are replaced by longitudinal rolls parallel to the flow in which shear is introduced. Suitability of the mathematical model for convective rolls has been discussed in Reference 7.

0271–2091/93/030217–14$12.00

Received May 1991
Revised September 1992

It is further noted that the motion of the flow in closed cells is upwards in the middle and down on the sides whereas for an open cell the motion is in the reverse.

The computations were carried out on a Burroughs 6700 with an average speed of 0·05 megaflops.

MATHEMATICAL MODEL

The non-dimensional system of equations for moist convection has been derived in Mann[8] for two-dimensional motion and found to be

$$\frac{\partial \eta}{\partial t} = J(\eta, \psi) - \frac{R}{\sigma}\frac{\partial T}{\partial x} + \nabla^2 \eta, \tag{1}$$

$$\frac{\partial T}{\partial t} = J(T, \psi) + S\frac{\partial \psi}{\partial x} + \frac{1}{\sigma}\nabla^2 T, \tag{2}$$

$$\eta = -\nabla^2 \psi, \tag{3}$$

where

ψ = streamfunction,
η = y-component of vorticity,
T = temperature,
x, z = rectangular axes,
g = gravitational acceleration,
T_0 = reference temperature,
ν = eddy viscosity,
κ = eddy thermal diffusivity,
ΔT = temperature difference across the layer,
S = latent heat factor,
d: layer thickness,
J: Jacobian,
$R = g\Delta T d^3/T_0 \kappa \nu$ is the Rayleigh number,
$\sigma = \nu/\kappa$ is the Prandtl number. (4)

The term including S in (2) provides the latent heat effects on the buoyancy drive in the development of cumulus clouds. The hydrostatic equation is used in the process of simplifying the equations. This is reasonable for non-rotating motion, particularly with a Boussinesq approximation.

The system operates for atmospheric cellular convection with a saturated updraught from the base. The system may be extended to include the conservation equations for water vapour and liquid water. The potential temperature model of Asai and Nakasuji[9] is similar to the independent derivation presented here. The potential temperature and absolute temperature models are equivalent for a shallow layer of the atmosphere. Van der Borght and Agee[2] used a moist model with an imposed hexagonal planform. For the case in which the region has a saturated updraught from the base, it can be shown that their model corresponds to that of this research. This simple model is appropriate for the initial stages of non-linear finite element modelling of moist atmospheric convection.

BOUNDARY CONDITIONS

A major difficulty in modelling atmospheric convection with a mathematical model, lies in the imposition of realistic boundaries. Laboratory models of atmospheric convection experience similar difficulties.

A rectangular domain has been chosen to enable comparisons to be made with various finite difference and approximation models. The horizontal extent $x \in [0, D]$ and the vertical height $z \in [0, 1]$ define this non-dimensional domain.

The lower boundary is uniformly maintained at a constant scaled temperature of zero with the upper boundary held at a non-dimensional temperature of -1. The lateral boundaries have zero heat flux across them. This may be interpreted as imposing periodicity, or, in the case of laboratory convection, as imposing insulated lateral boundaries. It may be assumed, without loss of generality, that the domain portrays one-half of a symmetric region of the atmosphere and, therefore, one lateral boundary condition on heat flux is quite valid. The imposition of the same condition on the other lateral boundary would seem to restrict the number of cells in a region to integer multiples of half-cells. However, there is difficulty in imposing a suitable replacement.

With the velocity of the fluid $\underset{\sim}{u} \equiv (u, w)$, the tangential viscous stress is zero on both upper and lower boundaries (free boundaries) giving

$$\frac{\partial u}{\partial z} = 0 \qquad \text{on } z = 0, 1 \tag{5}$$

or, using the continuity condition,

$$\frac{\partial^2 w}{\partial z^2} = 0 \qquad \text{on } z = 0, 1. \tag{6}$$

There is no flow across the upper and lower boundaries:

$$w = 0 \qquad \text{on } z = 0, 1. \tag{7a}$$

There is no mass flux across the lateral boundaries:

$$u = 0 \qquad \text{on } x = 0, D. \tag{7b}$$

No tangential viscous stress along the lateral boundaries implies

$$\frac{\partial w}{\partial x} = 0 \qquad \text{on } x = 0, D. \tag{8}$$

These may be readily converted to values for ψ and η and presented, with the above, in Table I.

It is noted that free boundaries are unrealizeable in a laboratory but are appropriate for large-scale geophysical phenomena where convection layers are most often bounded by a free surface or by a region of stable fluid.

LOCAL ANALYSIS AND PARAMETER VALUES

With the boundary conditions of Table I, the application of the local analysis of Chandrasekhar[10] and the use of a one-mode approximation, the marginal stability relationship for this system is found to be (Reference 7)

$$R = \frac{(\pi^2 + a^2)^3}{(S + \beta)a^2}, \tag{9}$$

Table I. Boundary conditions for the non-dimensional Boussinesq transient thermal convection

	u	$\frac{\partial u}{\partial z}$	w	$\frac{\partial w}{\partial x}$	T	$\frac{\partial T}{\partial x}$	$\frac{\partial T}{\partial z}$	ψ	η	$\frac{\partial^2 w}{\partial z^2}$
$z=0$		0	0		0			0	0	0
$z=1$		0	0		-1			0	0	0
$x=0$	0			0		0		0	0	
$x=D$	0			0		0		0	0	

where

$$a = \text{wavenumber of a cell},$$

$$\lambda = \frac{2\pi}{a} = \text{wavelength of a cell}, \tag{10}$$

$$\beta = \text{absolute linear temperature gradient}.$$

Obviously, equating S to zero, reverts the system to absolutely unstable convection. It is seen that R_c, the marginal value of the Rayleigh number for which convection occurs, is lowered with the inclusion of the moisture effects. Applying typical atmospheric values[8] gives a value of S at 20°C to be approximately 0·5. Asai and Kasahara[11] obtained this value for their potential temperature model and in describing the compensating downward motion of cumulus clouds assigned S a positive value for upward saturated motion and a similar negative value for the decreasing dry motion. Hence,

$$S = \begin{cases} 0{\cdot}5 & \text{for} \quad w > 0, \\ -0{\cdot}5 & \text{for} \quad w \leqq 0, \end{cases} \tag{11}$$

R is taken to be 10^4, a value at which the mathematical model is valid. This enables useful comparisons to be made with finite difference models, both quantitatively and qualitatively. The flow is quite non-linear at this value and so representative of the motion involved. The Prandtl is taken to be unity.

COMPUTATIONAL MODEL

Given the system

$$L\{\phi\} = 0, \tag{12}$$

where

$$L = \text{differential operator},$$

$$\phi = \text{unknown function}$$

and choosing ϕ_a as an unknown trial function within an element such that

$$\phi_a = \sum_{i=1}^{n} N_i \phi_i \tag{13}$$

where

$$\phi_i = \text{nodal values of function},$$

$$N_i = \text{appropriate shape function}, \tag{14}$$

$$n = \text{number of nodes in element},$$

then the finite element Galerkin criterion produces

$$\sum_{1}^{N_e} \iint_{A^{(e)}} N_j L\left(\sum_{i=1}^{n} N_i \phi_i\right) \mathrm{d}A^{(e)} = 0, \quad j = 1, \ldots, n, \tag{15}$$

where

$$\begin{aligned} A^{(e)} &= \text{area of element,} \\ N_e &= \text{the number of elements,} \\ N_j &= \text{weight function, shape function.} \end{aligned} \tag{16}$$

With time $j+1 = t_0 + (j+1)\Delta t$ being denoted by superscript $(j+1)$, and using an extension of the Taylor approximation outlined by Briley and McDonald[12] the Jacobian $J(\eta, \psi)^{j+1}$ may be approximated by

$$J(\eta,\psi)^{j+1} \approx \left(\frac{\partial \eta}{\partial x}\right)^{j}\left(\frac{\partial \psi}{\partial z}\right)^{j+1} + \left(\frac{\partial \psi}{\partial z}\right)^{j}\left(\frac{\partial \eta}{\partial x}\right)^{j+1} - \left(\frac{\partial \eta}{\partial z}\right)^{j}\left(\frac{\partial \psi}{\partial x}\right)^{j+1} - \left(\frac{\partial \psi}{\partial x}\right)^{j}\left(\frac{\partial \eta}{\partial z}\right)^{j+1} - J(\eta,\psi)^{j}. \tag{17}$$

The application of the finite element Galerkin criterion to the three-equation system (1)–(3) together with the use of Green's theorem on the Laplacian operator to reduce the order of the derivative and, hence, reduce the necessity for a higher-order shape function for the particular dependent variable, incorporating (17) and using the Crank–Nicolson algorithm produces the Finite Element Galerkin Green Taylor Crank–Nicolson (FEGGTC) system where values in the load matrix are from the previous time $j-1$

$$\begin{aligned} &\iint \left[\left(N^{\mathrm{T}} N \frac{2}{\Delta \mathrm{t}} + \left(N_x^{\mathrm{T}} N_x + N_z^{\mathrm{T}} N_z\right)\right)\{\eta\} + \frac{R}{\sigma} N^{\mathrm{T}} N_x \{T\} - N^{T} N_x \{\eta\}^{j-1} N_z \{\psi\}\right. \\ &\quad \left. - N^{\mathrm{T}} N_x \{\eta\} N_z \{\psi\}^{j-1} + N^{\mathrm{T}} N_x \{\psi\} N_z \{\eta\}^{j-1} + N^{\mathrm{T}} N_x \{\psi\}^{j-1} N_z \{\eta\}\right] \mathrm{d}x\, \mathrm{d}z - \int_l N^{\mathrm{T}} N_n \{\eta\}\, \mathrm{d}l \\ &= \iint \left[\left(N^{\mathrm{T}} N \frac{2}{\Delta t} - \left(N_x^{\mathrm{T}} N_x + N_z^{\mathrm{T}} N_z\right)\right)\{\eta\} - \frac{R}{\sigma} N^{\mathrm{T}} N_x \{T\}\right] \mathrm{d}x\, \mathrm{d}z + \int_l N^{\mathrm{T}} N_n \{\eta\}\, \mathrm{d}l, \end{aligned} \tag{18}$$

$$\begin{aligned} &\iint \left[\left(N^{\mathrm{T}} N \frac{2}{\Delta \mathrm{t}} + \frac{1}{\sigma}\left(N_x^{\mathrm{T}} N_x + N_z^{\mathrm{T}} N_z\right)\right)\{T\} - S N^{\mathrm{T}} N_x \{\psi\} - N^{T} N_x \{T\}^{j-1} N_z \{\psi\}\right. \\ &\quad \left. - N^{\mathrm{T}} N_x \{T\} N_z \{\psi\}^{j-1} + N^{\mathrm{T}} N_x \{\psi\} N_z \{T\}^{j-1} + N^{\mathrm{T}} N_x \{\psi\}^{j-1} N_z \{T\}\right] \mathrm{d}x\, \mathrm{d}z - \frac{1}{\sigma} \int_l N^{\mathrm{T}} N_n \{T\}\, \mathrm{d}l \\ &= \iint \left[\left(N^{\mathrm{T}} N \frac{2}{\Delta t} - \frac{1}{\sigma}\left(N_x^{\mathrm{T}} N_x + N_z^{\mathrm{T}} N_z\right)\right)\{T\} + S N^{\mathrm{T}} N_x \{\psi\}\right] \mathrm{d}x\, \mathrm{d}z + \frac{1}{\sigma} \int_l N^{\mathrm{T}} N_n \{T\}\, \mathrm{d}l, \end{aligned} \tag{19}$$

$$\begin{aligned} &\iint \left[-N^{\mathrm{T}} N \{\eta\} + \left(N_x^{T} N_x + N_z^{\mathrm{T}} N_z\right)\{\psi\}\right] \mathrm{d}x\, \mathrm{d}z - \int_l N^{\mathrm{T}} N_n \{\psi\}\, \mathrm{d}l \\ &= \iint \left[N^{\mathrm{T}} N \{\eta\} - \left(N_x^{T} N_x + N_z^{\mathrm{T}} N_z\right)\{\psi\}\right] \mathrm{d}x\, \mathrm{d}z + \int_l N^{\mathrm{T}} N_n \{\psi\}\, \mathrm{d}l, \end{aligned} \tag{20}$$

where

$$l = \text{contour of the boundary},$$

$$\{\psi\} = \begin{bmatrix} \psi_1 \\ \vdots \\ \psi_n \end{bmatrix} \quad \text{(similarly for } \{\eta\}, \{T\}), \tag{21}$$

$$N \equiv [N] = [N_1 \quad N_2 \quad \ldots \quad N_n], \tag{22}$$

$$S = \text{transpose } [S_1 \quad S_2 \quad \ldots \quad S_n] \tag{23}$$

and subscripts x and z refer to partial derivatives in those directions.

Due to the fact that the latent heat factor S only contributes on the upward motion and compensates on the downward motion and that in any one element the motion may be ascending at one node and descending at another, S needs to be included as a matrix. It is noted that in this model there is no Jacobian contribution to the 'load' matrix, due to cancellation.

RESULTS AND DISCUSSION

In the vertical plane, a rectangular region is analysed with the vertical $z{:}0 \rightarrow 1$ divided into Nz equal divisions and the horizontal $x{:}0 \rightarrow D$ divided into Nx equal divisions, the x and z extents being non-dimensional. This results in there being $(Nz \times Nx)$ nodes and $2(Nz-1)$ $(Nx-1)$ triangles. NNODES and NUMEL refer to the number of nodes and elements, respectively, while IDRYS = 0 is a code indicating that the temperature T includes both linear and non-linear parts.

The use of the streamfunction formulation has been shown extensively to produce superior results to the primitive variable formulation for both barotropic and baroclinic models. A great many of the atmospheric models use linear finite elements with linear triangular elements being used predominantly in barotropic models. This research illustrates that the modelling of turbulent thermal convection in the atmosphere with these elements is equally satisfactory. Staniforth[13] observes that it is usually less accurate and more costly to use parabolic elements rather than linear elements although there is no one approach that is optimal for all problems and all geometries. In further support of this model, domain and discretization he indicates that an unstaggered mesh only presents difficulties when used with the primitive variable formulation in the application to barotropic models. This research indicates that turbulent cellular convection is equally well-discretized with a regular mesh when the ψ–η formulation is used.

Because in atmospheric cellular convection the location of the gradients of greatest values is unknown – mainly because it is unknown how many cells should occur – different sized elements are not employed in general. Although it cannot be determined by finite elements how the fluid will convect in a domain of infinite horizontal extent, some insight may be gained by repeated computations for several different values of D, thereby gaining some information about the modal behaviour and providing a comparative analysis for the understanding of the physical phenomena.

In the atmosphere, cumulus convection frequently occurs in a conditionally unstable layer because of the release of water vapour. A conditionally unstable atmosphere is one which is unstable for saturated ascension and stable when unsaturated and for descension. The clouds are formed where the ascending motion occurs and cloud-free regions exist where the descending motion occurs. Cloud shape is defined by that part of the saturated region in which condensation occurs. Two-dimensional convective rolls, which simulate the cloud streets of the atmosphere, are preferred in a convecting layer with significant vertical shear in the horizontal wind. Hexagonal planforms occur primarily over the oceans or large bodies of water under conditions of weak

negligible wind shear in the atmospheric boundary layer. Sheu *et al.*[3] used a two-dimensional mathematical model to simulate the dynamics of this tesselation of hexagonal cells. Mesoscale cellular convection may occur as either open or closed cells which indicate descending motion with cloud-free centres or ascending motion with cloudy centres, respectively.

'Free' bounding surfaces, as detailed in Table I, are maintained for the moist convection model even though a more realistic boundary condition at sea level would need to be considered in a more detailed study. Kuo and Sun[14] have shown, however, that the use of the rigid boundary condition at the base is not required to achieve steady convection, and only serves to require a larger number of iterative time steps to achieve convection. Sasaki[15] notes that the dynamical boundary conditions are not the factors flattening the cells and shows that a specific thermal boundary condition which is more typical of the atmosphere than the constant temperature condition may attribute to an increase in the aspect ratio. He imposed a zero modulation in the heat flux at the upper and lower boundaries.

The dependence of the value of S on the vertical velocity implies that for this model its dependence on the mesh density is significant. In initial numerical trials, oscillations in the vertical velocity would no doubt be contributed to by the coarseness of the mesh. Condensation of water vapour takes place only in the ascending flow so that latent heat effects add to the buoyancy when the vertical velocity is upward and there is a compensating value of S for the downward motion. Sheu *et al.*[3] do not make this compensatory allowance for the downward flow. In this model it is assumed that water vapour is supplied enough to maintain the cloud layer saturated with water vapour against its decrease due to condensation. No evaporation takes place in the descending region. Yamasaki[16] noted that the most significant effect of liquid water is to reduce the intensity of the convection. It is assumed that condensed liquid water remains in the cloud without falling out as precipitation.

For comparison with the solution for the absolutely unstable atmosphere,[17] a horizontal extent of $D=1\frac{1}{3}$ is chosen with a very fine mesh density.

The transiency of the problem necessitates the imposition of initial conditions. Gresho *et al.*[18] assert that the flow may be initiated with any temperature field but that the velocity field must be solenoidal. In their finite difference models, Asai and Nakasuji[9] chose either random or sinusoidal temperature perturbations to initiate the flow. Comparisons are presented here of the following initialization schemes which all include $\psi=\eta=0$ everywhere:

(i) $T(x,z)=-10^{-3}\ \text{Random}(x,z), \quad 0<\text{Random}(x,z)<1$, everywhere except on $z=0$, (24)

(ii) $T(x,z)=-1$ everywhere except on $z=0$. (25)

These most appropriately simulate atmospheric conditions with the former producing a closed cell and the latter an open cell as for dry convection. This was discussed in Reference 17 as being a good simulation of the atmosphere. The closed cell and its various properties are illustrated in Figures 1 and 2 and the open cell with its properties is depicted in Figures 3 and 4. It is seen that the ascending region extends over a more narrow horizontal extent than the descending region and the velocities of the former are significantly larger in absolute values than those of the latter, preserving continuity of mass. As the profile of the horizontally averaged absolute vertical velocity indicates, the maximum velocity occurs in the upper half of the convection layer with the closed cell attaining a value of 17·9 while the open cell has a value of 18·9. The growth with time of the horizontally averaged vertical velocity at the mid-level of the convective layer indicates that steady state has been attained. It is noted that 'overshooting' again occurs. The maximum velocity of each cell is approximately 40, which is significantly less than that for the dry convection model.

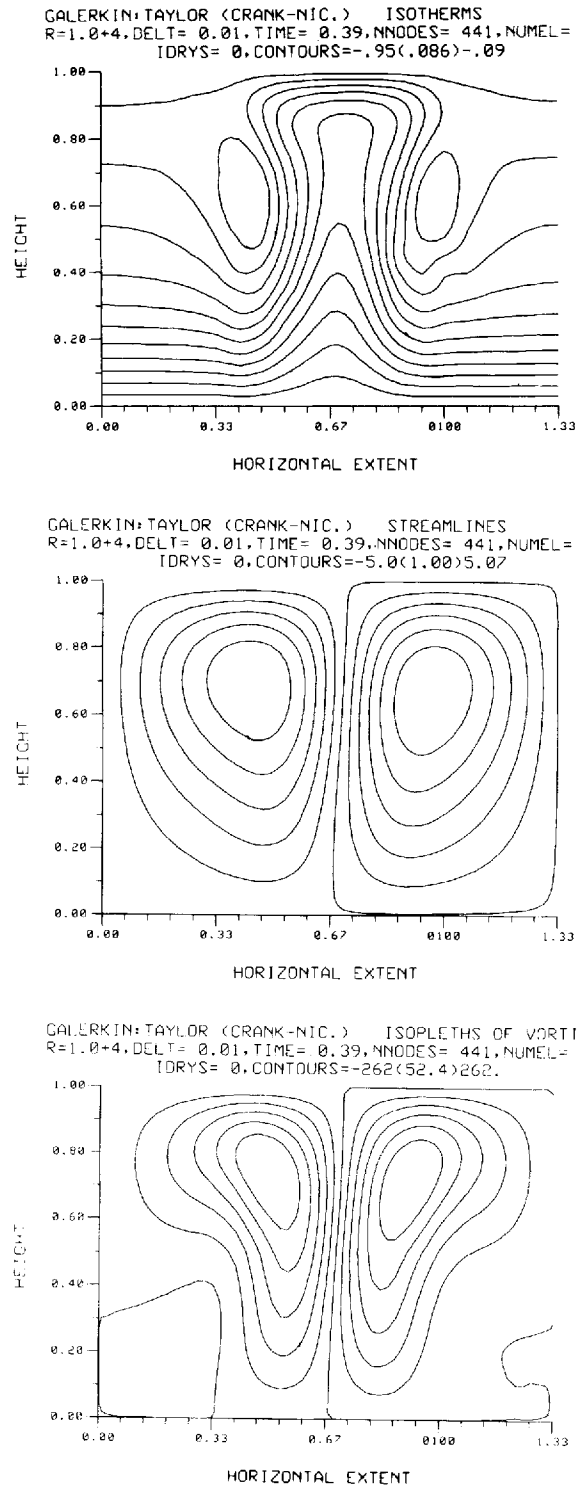

Figure 1. Isotherms, streamlines and vorticity isopleths for moist convection with initialization (24)

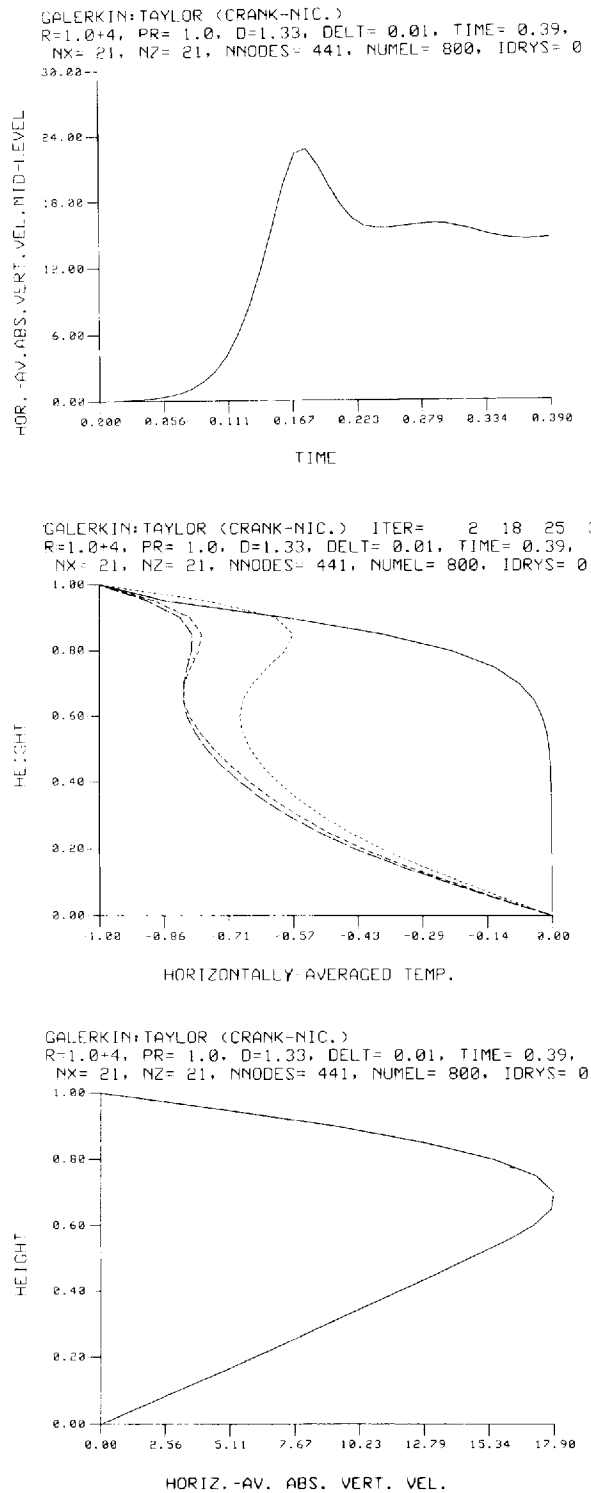

Figure 2. Vertical velocity and temperature profiles for moist convection with initialization (24)

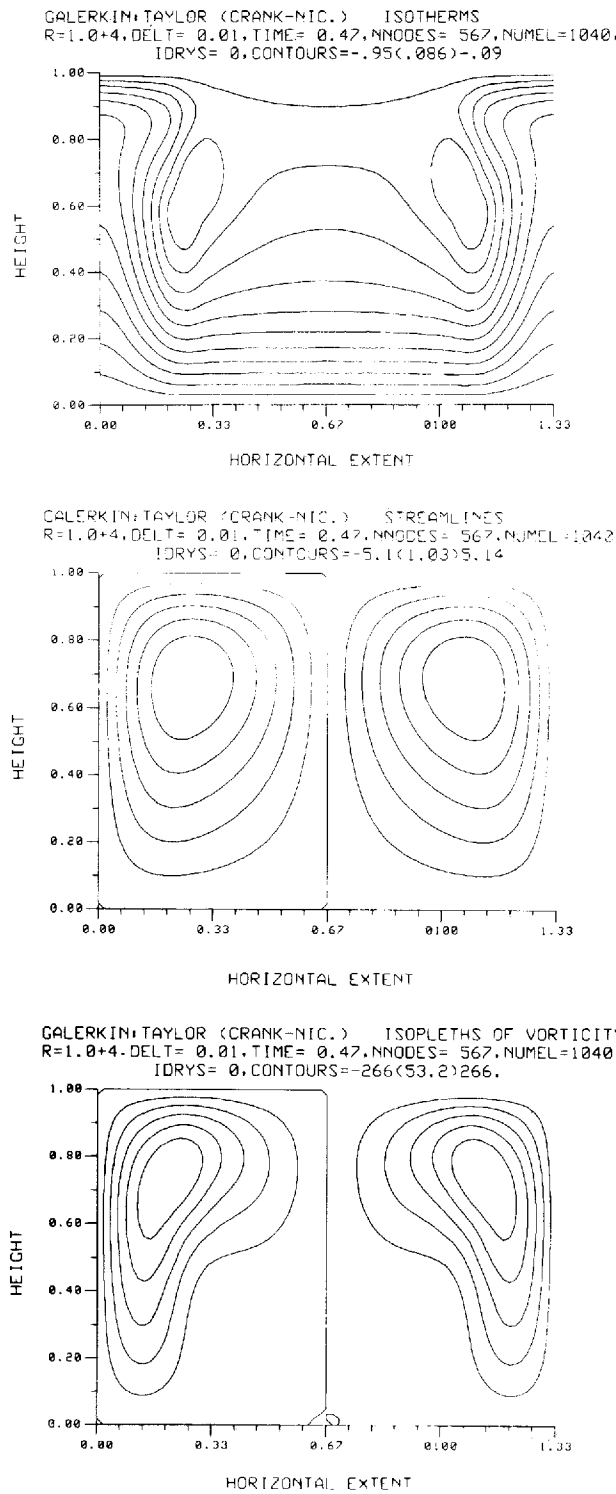

Figure 3. Isotherms, streamlines and vorticity isopleths for moist convection with initialization (25)

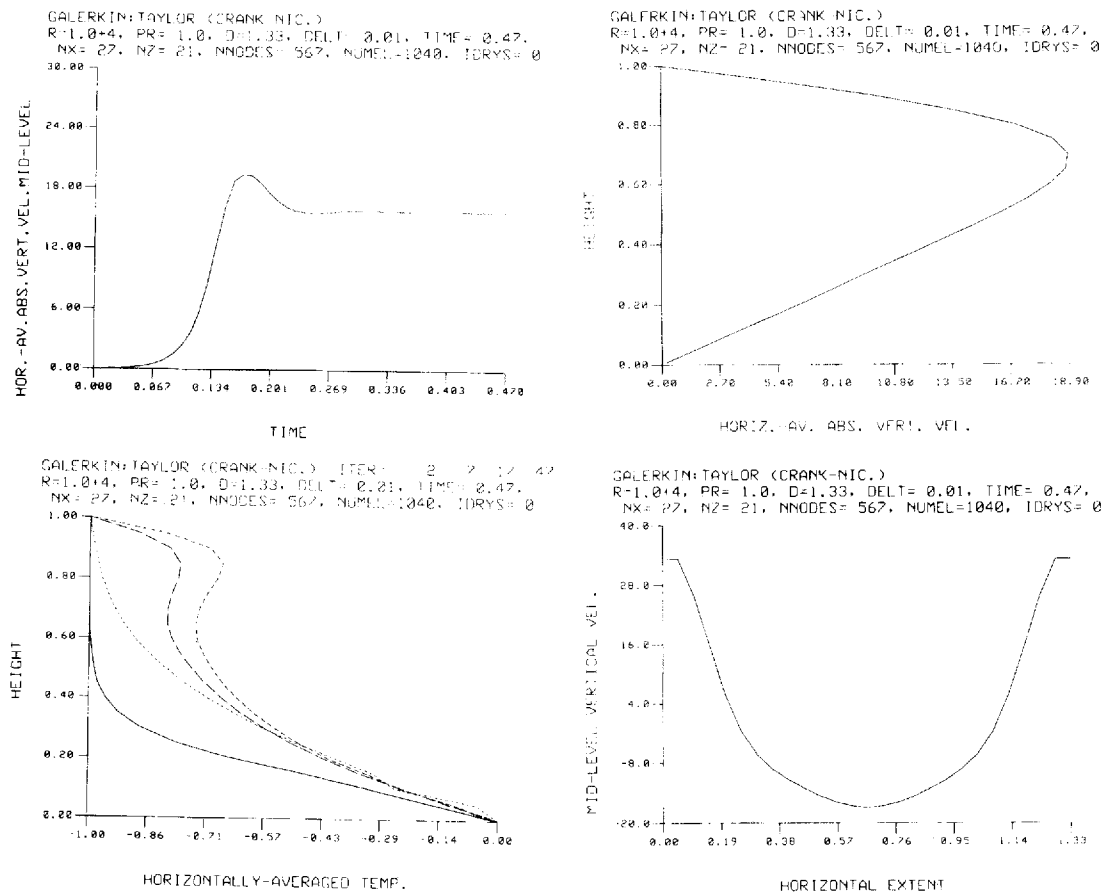

Figure 4. Vertical velocity and temperature profiles for moist convection with initialization (25)

The vertical profile of the horizontally averaged temperature exhibits a stable gradient in the upper portion of the convective layer. This is due to the inclusion of the latent heat effect. In (2), the term involving S indicates that the local rate of temperature increase is proportional to the magnitude of the upward vertical velocity.

The results so far illustrate that the model basically reproduces the physics of moist convection quite well. A larger domain is taken to provide a guide on the preferred mode.

Yamasaki[16] showed that the preferred size of an ascending area for which the growth rate is a maximum is uniquely determined while the growth rate increases with an increase in the descending area. The descending motion always acts as a stabilizing factor in the pseudo-adiabatic process in a conditionally unstable layer which is completely different from the convection in an absolutely unstable layer.

A horizontal extent of $D = 20{\cdot}0$ is taken to provide comparisons with the dry convection model. The various physical properties of the initial limited extent are again apparent with the additional property of an increased aspect ratio as illustrated in Figure 5. For dry convection, initialization (25) gave 9 open cells:[17] for this moist model there are approximately 5 open cells. Hence, the aspect ratio has increased from 2·2 to 4·0. For this domain, 151 horizontal grid points are used. In

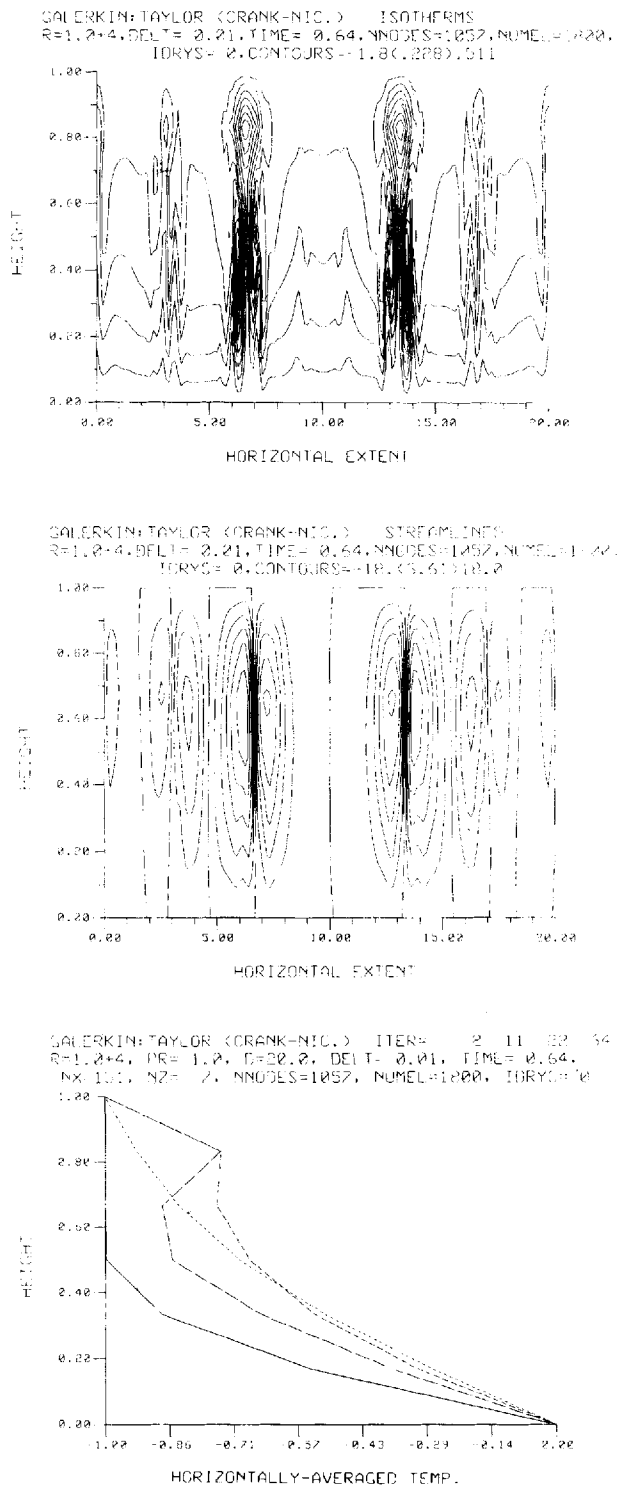

Figure 5. Moist convection with initialization (25) and $D = 20{\cdot}0$

their finite difference models, Sheu *et al.*[3] used 64 over $D=40{\cdot}0$ and Asai and Nakasuji[9] used $0{\cdot}2 \leq \Delta x \leq 0{\cdot}3$. The resultant value compares favourably with that of Asai and Nakasuji.

The marginal stability curve for dry convection as described by (9) with $S=0$, has marginal values of $R_c=657$, $a_c=2{\cdot}2$ and $\lambda_c=2{\cdot}8$ for the boundary conditions of this model. As (9) indicates, the inclusion of the latent heat effects lowers the marginal stability curve so that R_c is now less than 657 but that a_c and λ_c remain as before. This would then indicate that for a value of $R=10^4$ the convective vertical velocity should be greater for moist convection than for dry convection. However, the increasing of the aspect ratio of the convection cells which corresponds to decreasing the wavenumber to less than a_c would cause the marginal value of R for convection to be increased and, hence, reduce the convective vertical velocity at $R=10^4$. It is apparent, therefore, that the convective vertical velocity will decrease with increasing aspect ratio for a fixed value of S of the order of that in (11).

This mathematical model differs significantly from that of Van der Borght and Agee[2] in that the saturated updraught commences at the base, whereas their latent heat effects entered at a height determined by the conservation of moisture equation and they used a significantly larger value of R.

It is apparent that the inclusion of the moisture effects alters the structure of a cell to that of a narrow ascending region and a wider descending region with the former of larger velocities than the latter, and also alters the preferred mode of convection by increasing the aspect ratio. It, therefore, seems reasonable to conclude that the moisture effects contribute towards the aspect ratio of atmospheric convection cells, observed to be larger than the theory had predicted.

The results of this FEGGTC model of moist convection are evidence that this method may play a successful role in this field. From this simplified model, the research may now proceed to gradually incorporate such extensions as thermal boundary conditions similar to those of Sasaki[15] and Van der Borght and Agee[2], involve the additional conservation equations of water vapour and liquid water as in Asai and Nakamura[19] and allow for variations in depth of the convective cells and perhaps seek a subcell structure through applying varied values of R across the convective layer. The computer programs have been constructed in modules so that extension to cover further facets requires significantly less work than the original research.

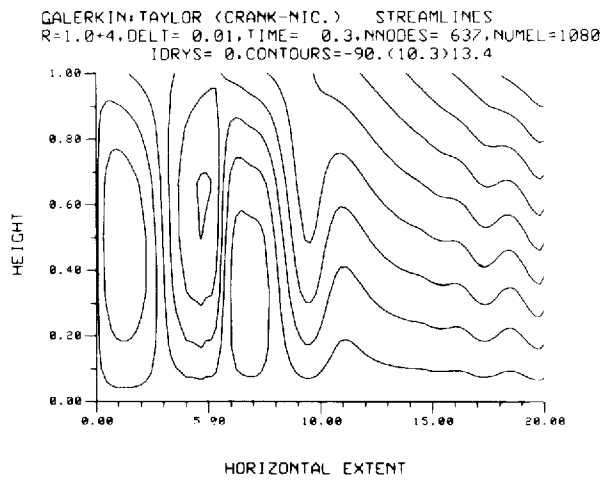

Figure 6. Moist convection with an imposed upward vertical velocity above the convective layer

For comparison with the finite difference model of Sheu *et al.*[3] a numerical experiment on the effect of large-scale vertical motion on moist convection was conducted. They have shown that simulation of a large-scale vertical motion above the convective layer by a uniform vertical velocity w_0 (up or down) may be implemented by altering the boundary conditions on ψ in this model to

$$\psi(x, 1) = w_0 x, \qquad \psi(x, 0) = 0, \tag{26}$$

$$\psi(0, z) = 0, \qquad \psi(D, z) = w_0 Dz, \tag{27}$$

thus, avoiding discontinuities and not destroying conservation properties. Although they used an anisotropic ratio of 400, qualitative comparisons may be made. For this trial, the upper boundary is insulated and initialization (25) is used. With an upward vertical velocity of 5 the quasi-steady cell structure of Figure 6 is depicted, illustrating an increase in the aspect ratio and also showing the inflow at the right lateral boundary balancing the net mass flux at the top of the layer due to the upward motion. Sheu *et al.* obtain a similar structure. It is also noted that apart from the dominance of this imposed vertical motion, the open-cell structure is maintained.

REFERENCES

1. E. M. Agee and K. E. Dowell, 'Observational studies of mesoscale cellular convection', *J. App. Meteorol.* **13,** 46–53 (1974).
2. R. Van der Borght and E. M. Agee, 'Nonlinear convection in a moist atmospheric layer heated from below', *J. Meteorol. Soc. Japan,* **56,** 284–292 (1978).
3. P. Sheu, E. M. Agee and J. J. Tribbia, 'A numerical study of physical processes affecting convective cellular geometry', *J. Meteorol. Soc. Japan,* **58,** 489–498 (1980).
4. K. Tsuchiya and T. Fujita, 'A satellite meteorological study of evaporation and cloud formation over the Western Pacific under the influence of the winter monsoon', *J. Meteorol. Soc. Japan,* **45,** 232–250 (1967).
5. D. Brunt, 'Experimental cloud formation', *Compendium Meteorol.,* 1255–1262 (1951).
6. H. L. Kuo, 'Perturbations of plane Couette flow in stratified fluid and the origin of cloud streets', *Phys. Fluids,* **6,** 195–211 (1963).
7. K. J. Mann, 'Computer simulations of atmospheric convection using finite elements', *Ph.D. Thesis,* Monash University, Melbourne, Australia, 1984.
8. K. J. Mann, 'Finite element modelling of atmospheric convection', *Proc. 3rd Int. Conf. on Finite Element Methods,* Sydney, 1979, pp. 713–729.
9. T. Asai and I. Nakasuji, 'On the preferred mode of cumulus convection in a conditionally unstable atmosphere', *J. Meteorol. Soc. Japan,* **55,** 151–167 (1977).
10. S. Chandrasekhar, *Hydrodynamic and Hydromagnetic Stability,* Oxford University Press, Oxford, 1961.
11. T. Asai and A. Kasahara, 'A theoretical study of the compensating downward motions associated with cumulus clouds', *J. Atmos. Sci.,* **24,** 487–496 (1967).
12. W. R. Briley and H. McDonald, 'Solution of the multidimensional compressible Navier Stokes equations by a generalised implicit method' *J. Comput. Phys.,* **24,** 372–397 (1977).
13. A. Staniforth, 'A review of the application of the finite element method to meteorological flows', in T. Kawai (ed.), *Finite Element Analysis,* Univ. of Tokyo Press, Tokyo, 1982.
14. H. L. Kuo and W. Y. Sun, 'Convection in the lower atmosphere and its effects', *J. Atmos. Sci.,* **33,** 21–40 (1976).
15. Y. Sasaki, 'Influences of thermal boundary layer on atmospheric cellular convection', *J. Meteorol. Soc. Japan,* **48,** 492–501 (1970).
16. M. Yamasaki, 'Finite amplitude convection in a conditionally unstable stratification', *J. Meteorol. Soc., Japan,* **52,** 365–379 (1974).
17. K. J. Mann, 'A computerised finite element model of the preferred mode in an absolutely unstable atmosphere', (submitted).
18. P. M. Gresho, R. L. Lee, S. T. Chan and R. L. Sani, 'Solution of the time-dependent incompressible Navier–Stokes and Boussinesq equations using the Galerkin finite element method', *Lawrence Livermore Lab. Preprint UCRL-82899,* 1979.
19. T. Asai and K. Nakamura, 'A numerical experiment of airmass transformation processes over warmer sea. Part 1. Development of a convectively mixed layer', *J. Meteorol. Soc., Japan,* **56,** 424–434 (1978).